COMBUSTION AND FLAME 38: 143-154 (1980)

Laminar Burning Velocity of Propane-Air Mixtures at High Temperature and Pressure

M. METGHALCHI* and J. C. KECK

Department of Mechanical Engineering, Massachusetts Institute of Technology, Cambridge, Massachusetts 02139

The laminar burning velocity of propane-air mixtures has been measured in the pressure range 0.4 to 40 atm and temperature range 298 to 750 K for equivalence ratios from 0.8 to 1.5. The measurements were made in a constant-volume spherical combustion bomb which could be heated to 500 K. A thermodynamic analysis was used to calculate the laminar burning velocity from a pressure time history of the combustion process. The measured values were correlated using both power law and exponential expressions.

INTRODUCTION

The laminar combustion properties of fossil fuels at high temperatures and pressures are of fundamental importance for analyzing and predicting the performance of internal combustion engines and power plant burners. Of particular interest is the laminar burning velocity which plays an essential role in determining:

1) the ignition delay which affects the spark advance and cycle-to-cycle fluctuations [1],
2) the thickness of the wall quench layers which are the primary source of unburned hydrocarbons and carbon monoxide [2], [3], and
3) the minimum ignition energy to ignite the charge [4] which affects the range of equivalence ratio over which an engine can be operated. Experimental laminar burning velocities can also be used to check theoretical combustion models and calculate apparent activation energies.

At the present time there is some information about the laminar burning velocities of propane-air mixtures at low pressures [5-11], but none in the range of pressure and temperature encountered in internal combustion engines and burners. The purpose of this paper is to describe a constant volume bomb facility for measuring laminar flame velocities and to present measurements for propane-air mixtures at high temperatures and pressures.

EXPERIMENTAL APPARATUS

A schematic diagram of the combustion bomb used for these measurements is shown in Fig. 1. It has an inside diameter of 15.24 cm and was designed to withstand a pressure of 700 atm. Standard 14 mm spark plugs with extended stainless steel electrodes were used to form the spark gap at the center of the bomb. A standard capacitive discharge ignition system in which the energy stored in the capacitors can be varied from a few millijoules to 2 Joules, was used for producing the spark.

A "black box" representation of the experimental facility is shown in Fig. 2. The bomb is located in an oven and can be heated electrically to a temperature of 500 K. Gaseous fuels and air are introduced through a high pressure line. Pure

---

* Visiting Assistant Professor, Department of Mechanical Engineering, Northeastern University.

Published by Elsevier North Holland, Inc.,
52 Vanderbilt Avenue, New York, NY 10017

0010-2180/80/050143+12$01.75

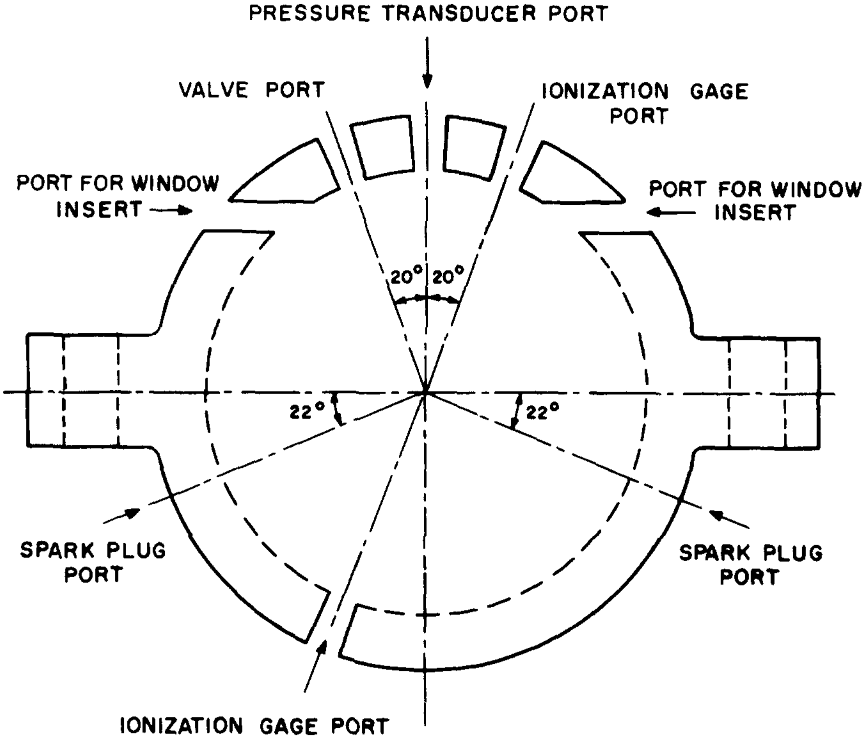

Fig. 1. Schematic diagram of the combustion bomb.

liquid fuels may be introduced as vapor. Wide boiling range fuels may be injected through a septum. Dynamic pressure was measured with a piezoelectric Kistler pressure transducer coated with silicon grease and calibrated against a balanced-pressure transducer on every run. This corrected the errors associated with the thermal sensitivity of the Kistler transducer. The arrival time of the flame front at the wall was measured using ionization probes located at three positions on the perimeter of the combustion bomb. These probes, which are flush with the spherical inner surface of the combustion bomb, were used to check for spherical symmetry of the flame.

For direct measurement of the flame front position a He-Ne laser system shown in Fig. 3 was used. The distance from center of the combustion bomb to the laser beam was 6.46 cm. When the flame front passes through the laser beam, a diffraction pattern similar to that produced by a knife edge is produced. The time when the flame front cuts the laser beam can be measured to ±0.1 msec and the radius of flame front can be measured to ±0.15 mm by using this system. A comparison of this radius with the corresponding value derived from pressure measurements is used to check the assumption of negligible preflame reactions made in the analysis of data.

Figure 4 shows the data handling and processing equipment used in the experiment. It consists of a two-channel 12 bit analog to digital converter controlled by a microcomputer. The maximum number of digitized points per channel is 256 and the time increment between two points is 0.25 msec. The instrumentation also includes four counters which are used to read the time when the three ionization probe pulses occur and the balanced-pressure switch closes. An oscilloscope is used to monitor all inputs.

To make a measurement the bomb was heated to the desired temperature and filled with the desired fuel/air mixture. A waiting time of 5 minutes was then allowed to permit the fuel and air to mix completely and become quiescent. To check that

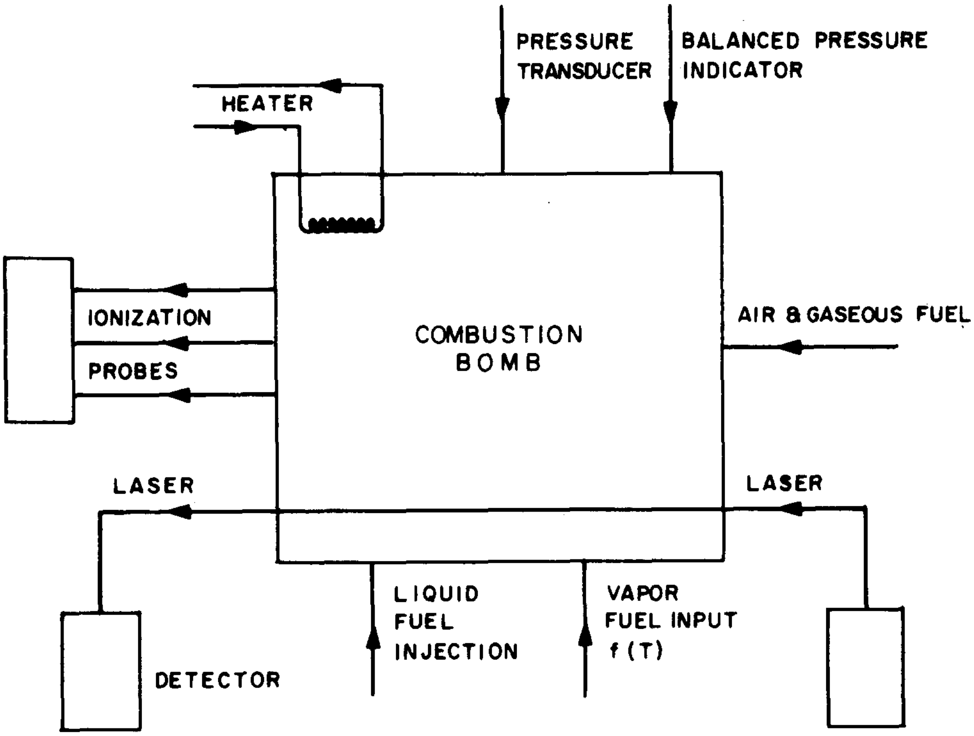

Fig. 2. Black box representation of the experimental facility.

this was sufficient, tests involving waiting times of 2 to 20 minutes were conducted. No effect on the measurement was observed and 5 minutes was chosen as a reasonable interval.

Figure 5 shows a typical oscillogram for a stoichiometric propane-air mixture having initial conditions of 1 atm. and 300 K. The horizontal scale is 10 msec/div. for pressure and ionization probe signals. The vertical scale for the pressure signal is 1.36 atm/div. The laser signal has been delayed 20 msec and the sweep rate is 1 msec/div.

The analog signals from the pressure transducer and the laser were fed directly to the microcomputer and the digitized data were transferred automatically from the microcomputer to the host computer. Times from the ionization probe and balanced pressure indicator counters were input manually to the host computer. The data could be processed immediately or stored in memory for later analysis.

THEORETICAL ANALYSIS

In the data reduction process the balanced-pressure indicator was first used to calibrate Kistler pressure transducer data. The dynamic pressure curves were then used to calculate the laminar burning velocity.

In the analysis of the data for a flame radius greater than 1 or 2 cm, it is a good approximation to assume that the thickness of the flame front is negligible and that the gas within the bomb consists of a burned fraction x at thermodynamic equilibrium and an unburned fraction $1 - x$ frozen at its original composition. It is further assumed that the pressure p is uniform, the flame front is smooth and spherical, the unburned gas is isentropically compressed, the heat loss is negligible and that there is no stratification of the charge.

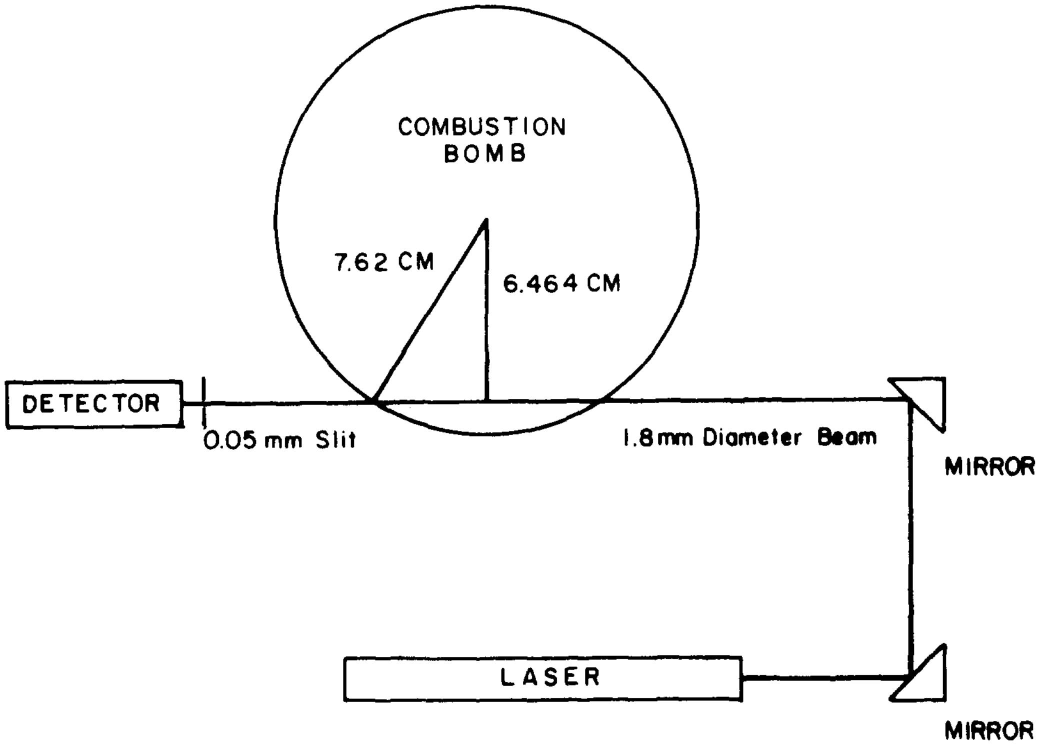

Fig. 3. Schematic diagram of laser system.

Under these conditions, the equations for conservation of volume and energy are

$$V/M = \int_0^x v_b \, dx' + \int_x^1 v_u \, dx' \tag{1}$$

$$E/M = \int_0^x e_b \, dx' + \int_x^1 e_u \, dx', \tag{2}$$

where

V = combustion bomb volume

M = mass of gas in the bomb

E = energy of gas in the bomb

v = specific volume

e = specific energy

and the subscripts b and u refer to burned and unburned gas, respectively.

For slowly varying burned gas specific heats, $v_b(T_b, p)$ and $e_b(T_b, p)$ may be expanded in a Taylor series about the mean burned gas temperature

$$\bar{T}_b = \frac{1}{x} \int_0^x T_b(x', x) \, dx'. \tag{3}$$

Neglecting terms of order $(T_b - \bar{T}_b)^2$ and higher, we find that Eqs. 1 and 2 become

$$V/M = x v_b(p, \bar{T}_b) + (1 - x) v_u(p, s_{u0}) \tag{4}$$

$$E/M = x e_b(p, \bar{T}_b) + (1 - x) e_u(p, s_{u0}). \tag{5}$$

The fractional error in x induced by this approximation is

$$\frac{\delta x}{x} \approx \frac{(\delta T_b)^2}{24 C_{vb}(\bar{T}_b - T_u)} \left(\frac{\partial C_{vb}}{\partial T} \right)_p, \tag{6}$$

where C_{vb} is the equilibrium specific heat of the burned gas at constant volume and δT_b is the

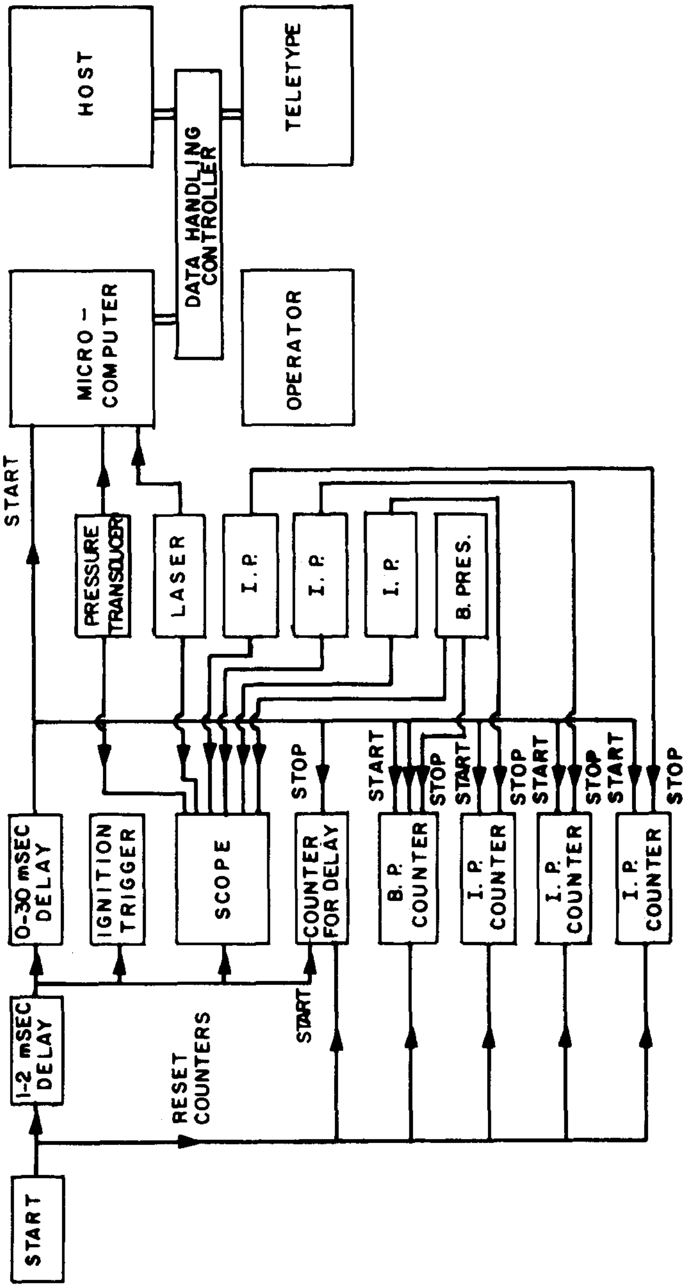

Fig. 4. Schematic diagram of data acquisition system.

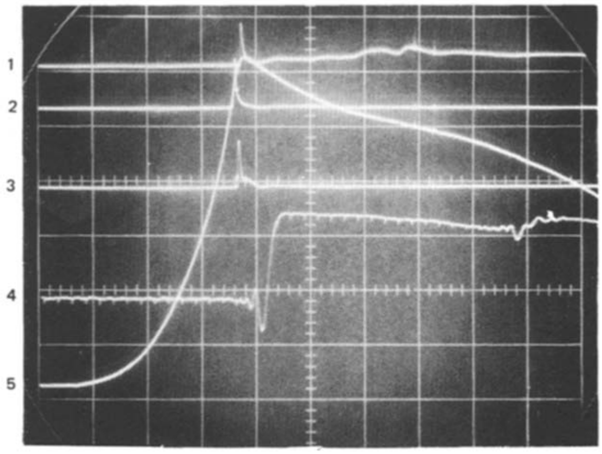

10 msec/div. Laser trace delayed 20 msec, sweep rate 1 msec/div.
Traces No. 1, 2 and 3: Ionization Probe Signals
Trace No. 4: Laser Signal
Trace No. 5: Pressure Transducer Signal

Fig. 5. A typical oscillogram for stoichiometric propane-air mixture.

spread in burned gas temperature. For the range of conditions investigated $\delta T \approx 500$ K and the corresponding value of $\delta x/x \leqslant .002$ which is negligible compared to measurement errors.

Equations 4 and 5 were solved for the two unknowns $\overline{T}_b$ and x using the Newton-Raphson, iteration method. The burned gas properties were computed using the equilibrium program of Martin and Heywood [12], and the unburned gas properties were computed using thermodynamic data from the JANAF Tables [13] and the assumption of frozen composition.

The following definitions result from the assumptions of spherical symmetry and mass conservation:

$$V_b = x\bar{v}_b M = (4/3)\pi R_f^3 \tag{7}$$

$$R_f = [3V_b/4\pi]^{1/3} \tag{8}$$

$$A_f = 4\pi R_f^2 \tag{9}$$

$$S_u = M\dot{x}(t)/\rho_u A_f \tag{10}$$

$$S_f = \dot{R}_f(t) \tag{11}$$

$$S_g = S_f - S_u, \tag{12}$$

where

R_f = radius of flame

A_f = area of flame

S_u = laminar burning velocity

$\dot{x}$ = rate of mass fraction burned

S_f = flame front velocity

S_g = unburned gas velocity at the flame front.

EXPERIMENTAL RESULT

Before undertaking extensive measurements a statistical study was made to check the reproducibility of data. Four identical runs for stoichiometric propane-air mixtures at an initial temperature of 298 K and 1 atm pressure were made and the laminar burning velocity was calculated along the isentropes for each. Fig. 6 shows the results plotted as a function of temperature and pressure. It can be seen that data are very reproducible.

Further evidence of the reproducibility is given in Table 1. The parameters shown are the peak

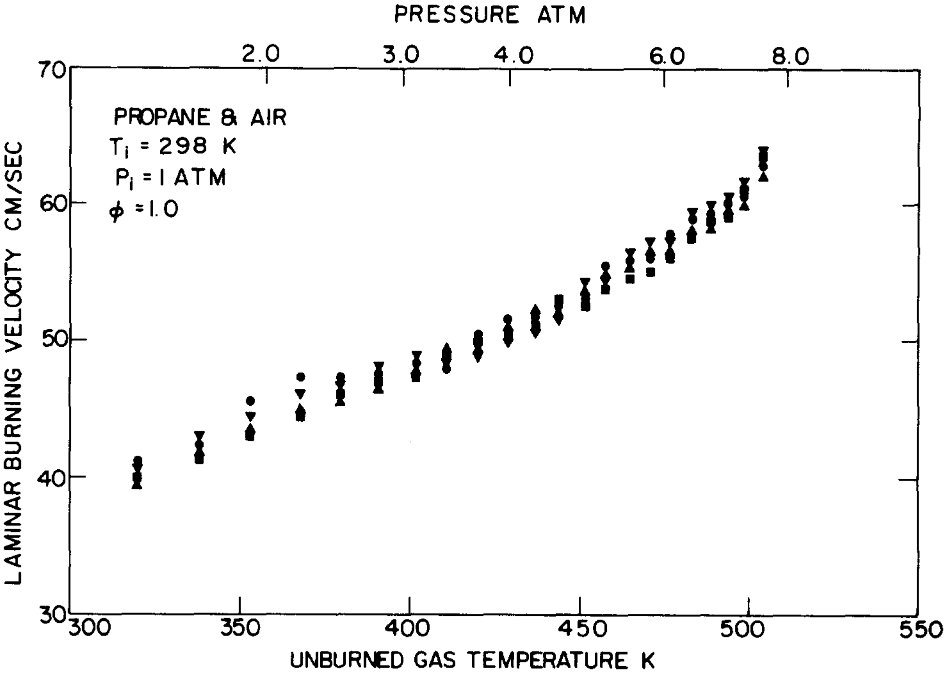

Fig. 6. Laminar burning velocity of stoichiometric propane-air mixture having atmospheric initial condition for four identical runs.

pressure p_p, the time at which peak pressure occurs t_p, the time deviation of the ionization probe pulse from the mean time $t_i - \bar{t}$, the standard deviation of flame radii deduced from the ionization probe pulses δR_{rms}, the deviation of the calculated flame front radius from that given by laser beam $\delta R_{\mathrm{laser}}$, and the unburned mass fraction burned at the end of combustion δx_u. As can be seen, the maximum pressures and the times at which maximum pressures occurred are very close for all four runs. Although there is some evidence of a systematic variation in the arrival times of the flame front at the ionization probes which might indicate a small asymmetry, it should be noted that since the flame speed is less than 100 cm/sec, the displacements involved are only fractions of a

TABLE 1

Run no.	p_p(atm)	t_p(msec)	$t_1 - t$ (msec)	$t_2 - t$ (msec)	$t_3 - t$ (msec)	δR_{rms}(mm)	$\delta R_{\mathrm{Laser}}$(mm)	δx_u
1	9.327	38.95	−0.32	0.68	−0.36	0.24	+0.004	0.001
2	9.135	39.21	−0.58	0.32	0.25	0.23	−0.069	0.025
3	9.210	39.21	−0.26	0.38	−0.11	0.15	−0.021	0.008
4	9.221	38.95	−0.49	0.45	−0.04	0.21	+0.019	0.015

p_p: Max. pressure

t_p: Time of p_p

$$\bar{t} = \frac{t_1 + t_2 + t_3}{3}$$

δR_{rms} : Std. diviation of I.P.

$\delta R_{\mathrm{Laser}} = R_{\mathrm{Calc}} - 6.464$

millimeter. This is smaller than the accuracy with which the probes could be positioned and is not considered significant. The other quantities in Table 1, δR_{rms}, $\delta R_{\mathrm{laser}}$, and δx_u, are all well within the accuracy of the measurements.

Systematic measurements of laminar burning velocities for propane-air mixtures were made at equivalence ratios of 0.8, 1.0, and 1.2. At each equivalence ratio, initial pressures of 0.4, 1.0, and 2.0 atm at room temperature were chosen. Measurements were first made along the isentropes starting at these initial conditions. They were then extended to higher temperatures and pressures by heating the bomb to 400 K and 500 K and choosing initial pressures that lie on the same isentropes. Laminar burning velocities were obtained for the pressure range 0.4-40 atm and temperature range 298 to 750 K by using this method.

Figure 7 shows the laminar burning velocity along one of these isentropes for a stoichiometric propane-air mixture having initial conditions of 296 K and 1 atm. Three overlapping runs are shown: the circle points have atmospheric initial conditions; the triangular points have initial conditions of 400 K and 3.13 atm, and the square points have initial conditions of 500 K and 7.6 atm. The scatter in data is less than ±2% and can be attributed to round off error in the analog to digital converter.

The temperatures at which ionization probe pulses occur are shown in the figure, and it can be seen that these probe pulses occur very close to each other.

The laminar burning velocity increases along an isentrope, peaks a little before peak pressure, and then falls off as the flame travels the last millimeter to the wall. The solid and dashed curves are two different fits to the data which will be described in the next section.

Figure 8 shows data for nine different isentropes. The top set is for propane-air mixtures with an equivalence ratio of 0.8, the second set is for stoichiometric mixtures, and the bottom set is for an equivalence ratio of 1.2. These data show that the laminar burning velocity decreases with increasing initial pressure at constant unburned gas temperature and increases with increasing unburned gas temperature at constant initial pressure.

Figure 9 shows the laminar burning velocity as a function of equivalence ratio for propane-air mixtures at a temperature of 298 K and pressure of 1 atm. The laminar burning velocity peaks for an equivalence ratio of 1.1 and falls off for both the rich and lean mixtures. The smooth curve is the best fit to polynomial of second degree. The equation for this curve is

$$S_{u0} = 38.31 + 24.84(\phi - 1) - 153(\phi - 1)^2. \quad (13)$$

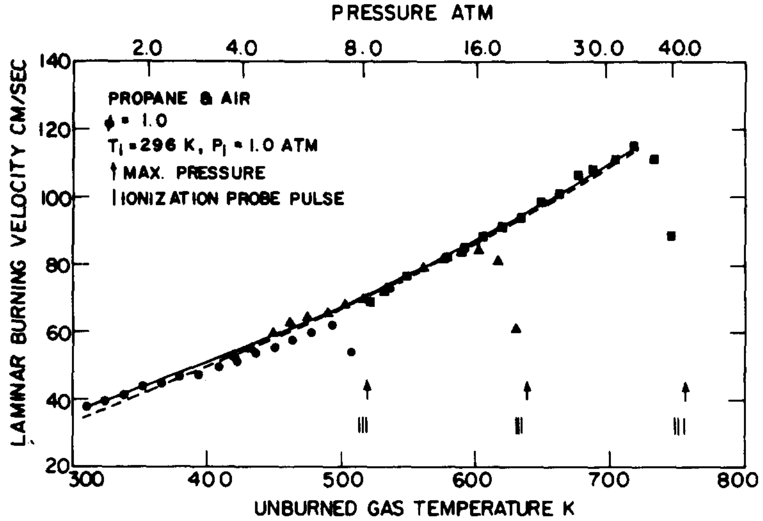

Fig. 7. Laminar burning velocity for stoichiometric propane-air mixtures.

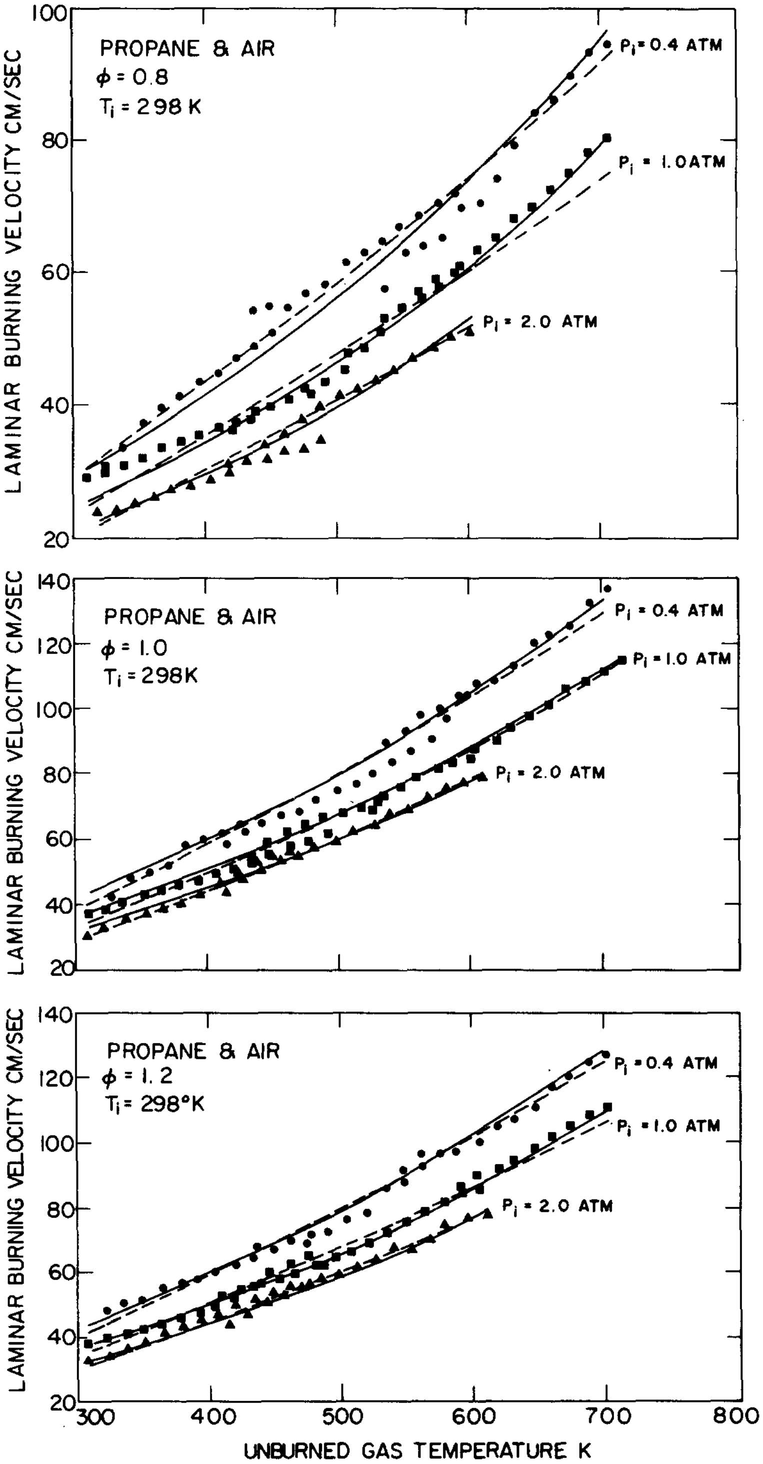

Fig. 8. Laminar burning velocity of propane-air mixtures at equivalence ratios of 0.8, 1.0, and 1.2.

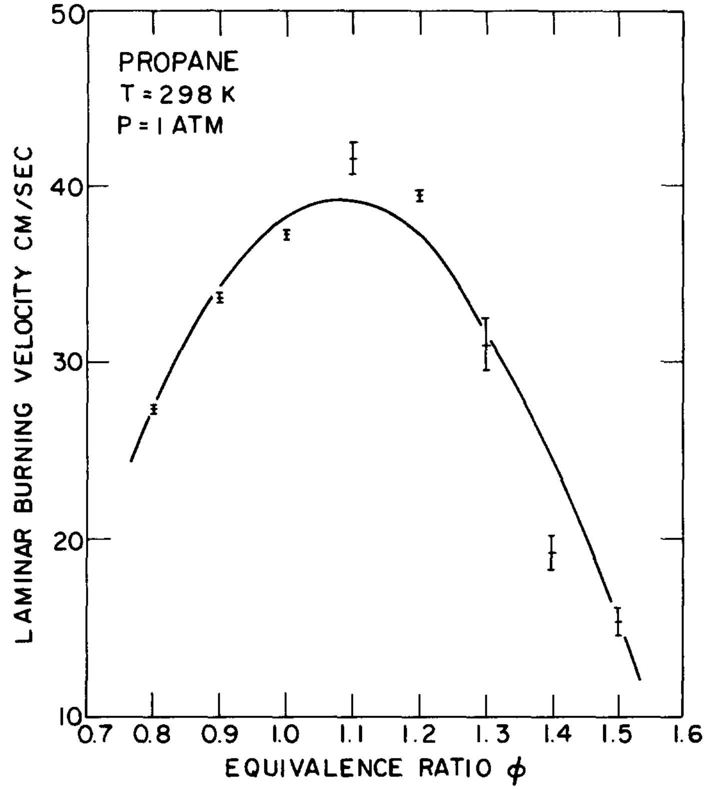

Fig. 9. Laminar burning velocity of propane-air mixture at atmospheric condition as a function of equivalence ratio.

DISCUSSIONS

The measured laminar burning velocities for propane-air mixtures have been fit to two different functional forms. The first is the simple power law relation

$$S_u = S_{u0}\left(\frac{T_u}{T_{u0}}\right)^{\alpha}\left(\frac{p}{p_0}\right)^{\beta}, \qquad (14)$$

where $T_{u0} = 298$ K and $p_0 = 1$ atm are the reference temperature and pressure and S_{u0}, α, and β are fitted constants. The values of S_{u0}, α, and β are given in Table 2 as a function of equivalence ratio along with the percentage δ_5 of data points falling within ±5% of the fitted curve. The power law fit (Eq. 14) is also shown graphically by the dashed curves in Figs. 7 and 8. For pressures above 2 atm the fit is quite good. Below 2 atm there appear to be some small systematic deviations.

The second relation used to fit the data is that used by Lavoie [13] to correlate data from previous experiments. It is given by

$$V_{\mathrm{STP}} \equiv \frac{\rho_u S_u}{\rho_{\mathrm{STP}}} = A\left(\frac{p}{p_0}\right)^{\beta} \exp\left(-E/2RT_b{}^{\circ}\right), \qquad (15)$$

where V_{STP} is the mass average burning velocity, $T_b{}^{\circ}$ is the adiabatic flame temperature and A, β, and E are fitted constants. The values of A, β, and E are given in Table 3 along with the percentage of data points within ±5 percent of the fitted curve.

The exponential fits (Eq. 15) are shown graphically by the solid curves in Figs. 7 and 8. It can be seen from these figures and the last columns in Tables 2 and 3 that the overall fit of the power law and exponential relations are about equally good. The exponential relation appears to be slightly better at pressures below 2 atm but it is very sensitive to the calculation of the adiabatic flame

TABLE 2

ϕ	S_{u0} cm/sec	α	β	Percent of data within ± 5%
0.8	23.3	2.27	−0.23	63
1.0	31.9	2.13	−0.17	74
1.2	33.8	2.02	−0.17	76

TABLE 3

ϕ	A cm/sec	β	E Cal/(gm.mole)	Percent of data within ±5%
0.8	17.1×10^4	0.757	72,500	62
1.0	136.8×10^4	0.713	95.600	74
1.2	6.98×10^4	0.803	66.900	88

temperature and much less convenient to use than the power law relation. There might be some tendency to prefer the exponential relation on fundamental grounds, however; in view of the strong variation of both the preexponential coefficient A and the apparent activation energy E with equivalence ratio, the physical significance of these quantities is extremely doubtful.

Comparison of the data in Table 3 with the corresponding values obtained by Lavoie [14] from previous data shows reasonable agreement for the pressure exponent but significant disagreement in the values of A and E. The most probable reason for this is the limited amount of high pressure and temperature data with which Lavoie had to work.

Figure 10 shows a comparison of laminar burning velocities measured in this study with those measured by Kuehl [5] as a function of the unburned gas temperature for stoichiometric propane-air mixtures at atmospheric condition. It can be seen that the difference is less than 8%. The variation of the reference laminar flame speed S_{u0} with equivalence ratio shown in Fig. 9 is also in good agreement with the low pressure data obtained by Kuehl.

Recent measurements of the burning velocity of propane-air mixtures made in a spherical bomb similar to that used in this study have also been reported by Ryan and Lestz [15]. Their results agree with ours at a temperature of 500 K and pressure of 6 atm but show a significantly steeper

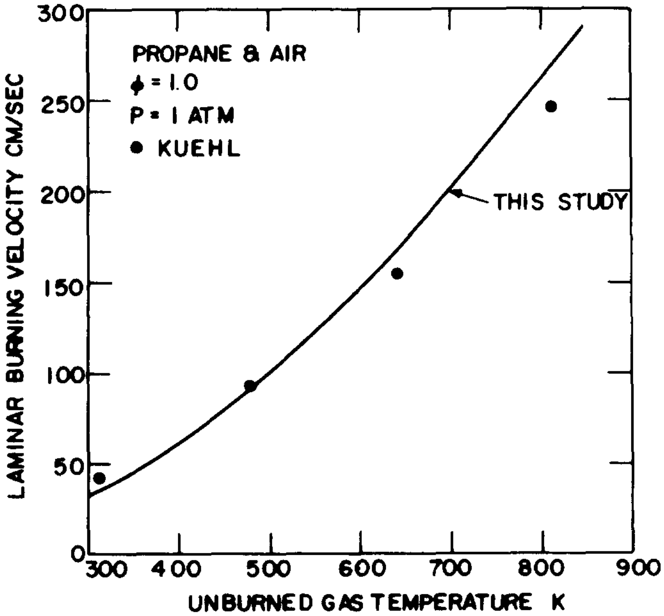

Fig. 10. Comparison of measured laminar burning velocity for propane-air mixture with those reported by Kuehl [5].

temperature dependence of the flame speed along an isentrope of the unburned gas. One possible reason for this is the assumption made by Ryan and Lestz that the volume consumed in each time step burns at constant volume. Since the combustion actually occurs at constant pressure, this leads to an incorrect value of the entropy for the burned gas which could in turn affect the calculated flame speeds.

On the basis of our experience we feel that the constant volume bomb technique of measuring adiabatic flame speeds is both efficient and accurate. Further refinements such as the use of interferometry [16] to measure unburned gas density, laser scattering to measure flame thickness, and the inclusion of wall heat transfer corrections have the potential to make it even more accurate.

Additional work with the bomb facility will include measurements of flame speeds for wide boiling range liquid fuels and studies of the effect of "residual gases" in the mixture.

The authors would like to thank Mr. Bob Dezmelyk and Professor William Unkel for invaluable assistance with the construction and installation of the on-line computer used in this work and Mr. Fee Yee for his assistance with the bomb hardware and electronics. The authors would also like to thank Professor C. J. Rallis of the University of Witwatersand for providing a number of very useful reports on the work of his group with the constant volume bomb. Initial phases of the work were supported by a Grant from the General Motors Corporation. Current support is being provided by Grants from the Army Research Office DAAG29-78-C-0010 and the National Science Foundation ENG77-14661.

REFERENCES

1. Blizard, N. C., and Keck, J. C., Paper 740191, presented at Automotive Engineering Congress, Detroit, February 1974.
2. Ferguson, C. R., and Keck, J. C., *Combust. Flame* 28:197–205 (1977).
3. Ferguson, C. R., and Keck, J. C., *Combust. Flame* 34:85–93 (1979).
4. DeSoete, G. G., *Thirteenth Symposium (International on Combustion,* 1972, p. 735.
5. Kuehl, D. K., *Eighth Symposium (International) on Combustion,* 1960, p. 510.
6. Brokaw, R. S., and Gerstein, M., *Sixth Symposium (International) on Combustion,* 1956, p. 66.
7. Kaskan, W. F., *Sixth Symposium (International) on Combustion,* 1956, p. 134.
8. Agnew, J. T., and Graiff, L. B., *Combust. Flame* 5: 209 (1961).
9. Chase, J. D., and Weinberg, F. J., *Proc. Royal Soc.* A275:411 (1962).
10. Raezer, S. D., and Olsen, H. L., *Combust. Flame* 6:227 (1962).
11. Dugger, G. L., and Grabb, D. D., *Fourth Symposium (International) on Combustion,* 1952, p. 302.
12. Martin, M. K., and Heywood, J. B., *Combust. Sci. Tech.* 15:1–10 (1977).
13. JANAF Thermochemical Tables, Dow Chemical Company, Clearinghouse, Springfield, VA.
14. Lavoie, G. A., Paper 780229, presented at Automotive Engineering Congress, Detroit, February-March 1978.
15. Ryan, T. W., and Lestz, S. S. Technical Paper CSS/CI-79-02. Central States Section of the Combustion Institute, April 1979.
16. Garforth, A. M., *Combust. Flame* 26:343–352 (1976).

Received 14 June 1979; revised and accepted 4 September 1979.